

Journal of Visualized Experiments

Development of efficient OLEDs from solution deposition

--Manuscript Draft--

Article Type:	Invited Methods Article - JoVE Produced Video
Manuscript Number:	JoVE61071R2
Full Title:	Development of efficient OLEDs from solution deposition
Section/Category:	JoVE Engineering
Keywords:	OLED; Solution Deposited Devices; Figures of Merit and Roll-off; Organic Electronics Engineering; Thermally Activated Delayed Fluorescence; Low-complex Device Structure; Simple OLED Fabrication Process
Corresponding Author:	Luiz Pereira Universidade de Aveiro Aveiro, PORTUGAL
Corresponding Author's Institution:	Universidade de Aveiro
Corresponding Author E-Mail:	luiz@ua.pt
Order of Authors:	Manish Kumar Luiz Pereira
Additional Information:	
Question	Response
Please indicate whether this article will be Standard Access or Open Access.	Standard Access (US\$2,400)
Please indicate the city, state/province, and country where this article will be filmed . Please do not use abbreviations.	Aveiro, Portugal

TITLE:

Development of Efficient OLEDs from Solution Deposition

AUTHORS AND AFFILIATIONS:

Manish Kumar^{1,2}, Luiz Pereira¹

¹Department of Physics and i3N, Institute for Nanostructures, Nanomodulation and Nanofabrication, University of Aveiro, Aveiro, Portugal

²CeNTI, Centre for Nanotechnologies and Smart Materials, R. Fernando Mesquita, Vila Nova de Famalicão, Portugal

*Both authors contributed equally.

Corresponding Author:

Luiz Pereira (luiz@ua.pt)

Email Address of Co-author:

Manish Kumar (mkumar@ua.pt)

KEYWORDS:

OLED, solution deposited devices, figures of merit roll-off, organic electronics engineering, thermally activated delayed fluorescence, low-complex device structure, simple OLED fabrication process

SUMMARY:

Presented here is a protocol for the fabrication of efficient, simple, solution-deposited organic light-emitting diodes with low roll-off.

ABSTRACT:

The use of highly efficient organic emitters based on the thermally activated delayed fluorescence (TADF) concept is interesting due to their 100% internal quantum efficiency. Presented here is a solution deposition method for the fabrication of efficient organic light-emitting diodes (OLEDs) based on a TADF emitter in a simple device structure. This fast, low-cost, and efficient process can be used for all OLED emissive layers that follow the host-guest concept. The fundamental steps are described along with necessary information for further reproduction. The goal to establish a general protocol that can be easily adapted for principal organic emitters currently under study and development.

INTRODUCTION:

The increase in organic electronics used in daily life has become an unsurpassed reality. Among several organic electronic applications, OLEDs are perhaps the most attractive. Their image quality, resolution, and color purity have made OLEDs a primary choice for displays. Moreover, the possibility to achieve large area emission in extremely thin, flexible, lightweight, and easy color-tunable OLEDs has applications in lighting. However, some technological issues associated with the fabrication process in large area emitters have postponed further application.

With the first OLED working at low applied voltages¹, new paradigms for solid-state lighting have been designed, though with low external quantum efficiency (EQE). The OLED EQE is obtained by the ratio of emitted photons (light) to injected electrical carriers (electrical current). A simple theoretical estimate for the maximum expected EQE is equal to $\eta_{out} \times \eta_{int}$ ². The internal efficiency (η_{int}) can be approximated by $\eta_{int} = \gamma \times \eta_{ST} \times \Phi_{PL}$, where γ corresponds to the charge balance factor, Φ_{PL} is the photoluminescence quantum yield (PLQY), and η_{ST} is the efficiency of emissive exciton (electron hole pair) generation. Finally, η_{out} is the outcoupling efficiency². If outcoupling is not considered, attention is focused on three topics: (1) how efficient the material is in creating excitons that radiatively recombine, (2) how efficient the emissive layers are, and (3) how efficient the device structure is in promoting a well-balanced electrical system³.

A purely fluorescent organic emitter has only 25% internal quantum efficiency (IQE). According to spin rules, the radiative transition from a triplet to a singlet (T→S) is forbidden⁴. Therefore, 75% of excited electrical carriers do not contribute to the emission of photons⁵. This issue was first overcome using transition metals in organic emitter phosphorescence OLEDs⁶⁻¹⁰, where the IQE was reportedly close to 100%¹¹⁻¹⁶. This is due to the spin-orbit coupling between the organic compound and heavy transition metal. The disadvantage in such emitters is their high cost and poor stability. Recently, reports on the chemical synthesis of a pure organic compound with low energy separation between the excited triplet and singlet states (ΔE_{ST}) by Adachi^{17,18} have given rise to a new framework. Although not new¹⁹, the successful employment of the TADF process in OLEDs have made it possible to obtain high efficiencies without using transition metal complexes.

In such metal-free organic emitters, there is a high probability for the excited carriers in a triplet state to populate to the singlet state; therefore, the IQE can achieve a theoretical limit of 100%^{5,20-22}. These TADF materials provide excitons that can radiatively recombine. However, these emitters require dispersion in a matrix host to avoid emission quenching^{3,20,21,23,24} in a host-guest concept. Additionally, its efficiency depends on how the host (organic matrix) is appropriated to the guest (TADF) material²⁵. Also, it is necessary to idealize the device structure (i.e., thin layers, materials, and thickness) to achieve an electrically balanced device (equilibrium between holes and electrons to avoid loss)²⁶. Achieving the best host-guest system for an electrically balanced device is fundamental to increase the EQE. In TADF-based systems, this is not simple, due to the changes in the electrical carrier mobilities in EML that are not easily tuned.

With TADF emitters, EQE values greater than 20% are easy to obtain²⁶⁻²⁹. However, the device structure is typically comprised of three to five organic layers (hole transport/blocking and electron transport/blocking layers, HTL/HBL and ETL/EBL, respectively). Additionally, it is fabricated using a thermal evaporation process that is high in cost, technologically complex, and almost only for display applications. Depending on the HOMO (highest occupied molecular orbital) and LUMO (lowest unoccupied molecular orbital) levels, electrical mobility of carriers, and thickness, each layer can inject, transport, and block electrical carriers and guarantee recombination in the emissive layer (EML).

Reducing the device complexity (e.g., a simple, two layer structure) usually results in a

noticeable decrease of EQE, sometimes to less than 5%. This happens due to the different electron and hole mobility in the EML, and the device becomes electrically unbalanced. Thus, instead of the high efficiency of exciton creation, the efficiency of emission in the EML becomes low. Moreover, a noticeable roll-off occurs with a strong decrease of the EQE as the brightness increases, due to the high concentration of excitons at a high applied voltage and long excited lifetimes^{24,30,31}. Overcoming such issues requires a strong capability to manipulate electrical properties of the emissive layer. For a simple OLED architecture using solution-deposited methods, electrical properties of the EML can be tuned by the solution preparation and deposition parameters³².

Solution deposition methods for organic-based devices have been previously used³¹. OLED fabrication, compared to the thermal evaporation process, is of great interest due to their simplified structure, low cost, and large area production. With high success in transition metal complexes OLEDs, the main goal is to increase the emitting area but keep device structure as simple as possible³³. Methods such as roll-to-roll (R2R)³⁴⁻³⁶, inkjet printing³⁷⁻³⁹ and slot-die⁴⁰ have been successfully applied in multilayer fabrication of OLEDs, which is a possible industrial approach.

Despite solution deposition methods for organic layers serving as a good choice for device architecture simplification, not all desired materials can be easily deposited. Two types of materials are used: small molecules and polymers. In solution deposition methods, small molecules have some drawbacks, such as poor thin film uniformity, crystallization, and stability. Thus, polymers are mostly used due to the ability to form uniform thin films with low surface roughness and on large, flexible substrates. Moreover, the materials should have good solubility in the appropriate solvent (mainly organic ones like chloroform, chlorobenzene, dichlorobenzene, etc.), water, or alcohol derivatives.

Besides the problem of solubility, it is necessary to guarantee that a solvent used in one layer should not act as one for the preceding layer. This allows a multi-layer structure deposited by the wet process; however, there are limitations⁴¹. The most typical device structure uses some solution-deposited layers (i.e., the emissive one) and one thermally evaporated layer (ETL). Additionally, thin film homogeneity and morphology strongly depend on the deposition methods and parameters. Electrical charge transport through these layers is completely governed by such morphology. Nevertheless, a tradeoff between the desired final device and compatibilities of the fabrication process should be judiciously established. Adjusting the deposition parameters is a key to success, despite being time-consuming work. For instance, the spin coating is not a straightforward technique. Although it seems simple, there are several aspects of thin film formation from a solution on top of a spinning substrate that require attention.

Besides film thickness optimization, manipulation of spinning velocity, and time (thickness is an exponential decay of both parameters), the experimenter's actions must also be adjusted to obtain good results. Correct parameters also depend on the solution viscosity, deposition area, and wettability/contact angle of solution on the substrate. There are no unique sets of parameters. Only basic assumptions with specific adjustments to the solution/substrate yield the desired results. Moreover, the electrical properties that depend on the layer molecular conformation and morphology can be optimized for desired results, following the

protocol described here. Once completed, the process is simple and feasible.

Nevertheless, decreasing the device structure complexity leads to a maximum EQE decrease; although, a compromise can be achieved in terms of efficiency vs. brightness. As such a compromise allows practical applications, the surplus of a simple, large area compatible, and low cost process can become a reality. This article describes these requirements and how to develop a recipe to handle the required issues.

The protocol focuses on a green TADF emitter 2PXZ-OXD [2,5-bis(4-(10H-phenoxazin-10-yl)phenyl)-1,3,4-oxadiazole]⁴² as a guest in a host matrix composed by PVK [poly(N-vinylcarbazole)] and OXD-7 [1,3-Bis[2-(4-tert-butylphenyl)-1,3,4-oxadiazole-5-yl]benzene], which corresponds to the EML. An electron transport layer (ETL) of TmPyPb [1,3,5-Tri(m-pyridin-3-ylphenyl)benzene] is used. Both the anode's and cathode's work functions are optimized. The anode is comprised of ITO (indium tin oxide) with a high conductive polymer PEDOT:PSS [poly(3,4-ethylenedioxythiophene)-poly(styrenesulfonate)], and the cathode is comprised of a double layer of aluminum and LiF (lithium fluoride).

Finally, both the PEDOT:PSS and EML (PVK: OXD-7: 2PXZ-OXD) are deposited by spin coating, whereas TmPyPb, LiF, and Al are thermally evaporated. Considering the conductive metal-like nature of PEDOT:PSS, the device is a typical "two organic layer" in the simplest structure possible. In the EML, TADF guest (10% wt.) is dispersed in the host (90% wt.) composed of PVK_{0.6}+OXD-7_{0.4}.

PROTOCOL:

CAUTION: The following steps involve the use of different solvents and organic materials, so proper care must be taken when handling. Use the fume hood and protective equipment such as lab glasses, face masks, gloves, and lab coats. Weighing of the materials should be done precisely using a high precision scale machine. To ensure cleanliness of the substrates, solution deposition of thin films, and evaporation, it is recommended that all the procedures be performed in a controlled environment or glovebox. Before the use of a spin-coater, micropipettes, thermal evaporators, organic materials, and solvents, all safety data sheets must be consulted.

1) Preparation of host-guest solution

1.1 In two small vials (volume between 4–6 mL, cleaned with isopropanol and dried with nitrogen), weigh host matrix composed of 12 mg of PVK and 8 mg of OXD-7. Start with weighing the OXD-7. Compensate any deviation in the weight using PVK to achieve a final ratio of 6:4 (PVK:OXD-7). In the second vial, weigh 10 mg of 2PXZ-OXD TADF emitter.

1.2 Add 2 mL of chlorobenzene to the vial with host matrix, and 1 mL to the vial with TADF material. If the weights of any vials are not exactly the values described above, adjust the chlorobenzene volume in both vials to achieve a solution with final concentration of 10 mg/mL.

1.3 Leave the solutions stirring with small, cleaned magnetic stir bars for at least 3 h to

ensure complete dissolution of the materials. Ensure that the vials are safely covered with respective caps and tightly sealed with organic chemical safe film to avoid any evaporation of solvents.

2. Substrate cleaning

NOTE: To handle the substrates, use a pair of tweezers, touching only in a corner (never touch the middle of the substrates). The substrates used here have six pre-patterned ITO pixels (**Figure 1A**).

2.1 Obtain pre-patterned ITO substrates. Clean substrates in an ultrasonic bath containing 1% v/v Hellmanex solution in water, acetone, and 2-propanol (IPA), sequentially, for 15 min in each bath. Perform the first bath at approximately 95 °C and the remaining at room temperature (RT). Finally, dry the substrates using nitrogen flux to remove any cleaning solvent residue.

2.2 Before fabrication, expose the substrates (ITO film facing upwards) to UV ozone treatment for 5 min. Carefully extract the gases and ensure that the ITO patterned face is exposed to the UV. Here, use an ozone cleaner (100 W, 40 kHz). Set the emission wavelength of the UV lamps to 185 nm and 254 nm with a high intensity, low pressure, mercury vapor discharge lamp.

3. Spin coating

This is the most important step of this protocol. To ensure uniformity, homogeneity, and absence of pinholes in the thin films, all solvents must be filtered with their respective filter papers. Complete removal of excess solvents from substrates should be ensured to avoid any short in the final device. For the substrates used here, the removal of excess materials from the patterned ITO and cathode is also important to fix the final pixel, and it should be performed with high precision, without disturbing the active area of the pixel. The steps described below should be followed for spin coating of the thin films. The final thickness of the thin film will vary if using a spin coater different than the one used here.

3.1 Prepare the spin coater equipment.

NOTE: Before using the spin coater, it is necessary to make a curve calibration with the deposition parameters and final thickness obtained for the films. This should be done for each solution employed. The procedure involves making several depositions for the same solution but with different parameters, and the final thickness is measured with a profilometer. **Figure 2** shows a typical calibration curve for an active layer.

3.2 Deposit PEDOT:PSS as the first layer on top of ITO. Filter the PEDOT:PSS with a 0.45 μm polyvinylidene fluoride (PVDF) filter. Fill a micropipet with 100 μL of PEDOT:PSS.

3.3 Carefully place the substrate on the spin coater chuck and activate the vacuum system to fix the substrate (**Figure 1B,C**). Rotate the ITO face-up and adjust to center the substrate area as much as possible. Set the parameters for the spin coating to 3,000 rpm for

30 s. Set an initial step using the spin coater of ~2–3 s at low rotation (200–500 rpm). A thickness of 30 nm is expected.

3.4 Keeping the micropipet perpendicular to the substrate (**Figure 1D**), drop the solution (100 μ L) in the middle of the substrate (**Figure 1D**) and start the spin coater (**Figure 1E**).

NOTE: Do not drop the solution too quickly or slowly to avoid the risk of nonhomogeneous spread of the solution (depending on the viscosity, the contact angle can be nonideal). Usually, dropping the solution in ~1 s is ideal. Do not touch the substrate with the micropipette, and try to synchronize between starting the spin coater and dropping the solution. If a two-step deposition setting (as explained in step 3.3) is not available, consider a static deposition: drop the solution first, then start the spin coater immediately after. Dropping of the solution should be done carefully. All solutions should be dropped at the center of the rotation axis and form a uniform spot to avoid nonuniformities during the process. Be advised that, although these rules are ideal for good film deposition, the spin coating technique is hard to optimize (i.e., requires several preoptimization steps). Furthermore, it depends on solution viscosity, deposition desired area, how the solution is dropped on the substrate, and the start of spinning. An example of good film formation at a microscopic scale can be seen in **Figure 3** as an AFM image.

3.5 Complete the spin coater step (**Figure 1F**). Turn off the vacuum, and with a tweezer, remove the substrate. With the help of small cotton bud soaked in water (i.e., the PEDOT:PSS solvent; **Figure 1G**), remove the excess deposited film around the cathode and corner areas from the substrate, keeping the central pixelated area untouched.

3.6 Keep the substrate in an oven or on a hot plate at 120 °C for 15 min to remove the PEDOT:PSS solvent (water). Remove from the oven or hot plate, move to a glovebox, and leave to cool down to RT (**Figure 1H**).

3.7 Prepare the solution for the EML. In a new clean vial (see step 1.1), using a micropipette, prepare a new solution composed of 1.8 mL of host solution and 0.2 mL of TADF solution. Before using the solution, filter it with a 0.1 μ m PTFE filter.

3.8 Leave the new solution stirring for 15 min at RT.

3.9 Following steps 3.3–3.5, make the deposition of this second solution in a spin coater in the glovebox. Spin at 2,000 rpm for 60 s. The expected film thickness should be 50 nm. To remove any excess of the second film, use cotton buds soaked in chlorobenzene.

3.10 Leave the substrates on a hot plate inside the glove box at 70 °C for 30 min to completely remove the excess chlorobenzene.

3.11 Remove the substrates from the hot plate and leave to cool to RT.

3.12 For additional precautions, consider some temperature/time (indirectly, evaporation rate) tests for different solvents. The morphology of the final film is strongly dependent on

these parameters. A simple AFM test can be useful to confirm that the solvent evaporation rate is adequate. The final structure of the deposited thin films should be more or less similar to the scheme in **Figure 11**.

4. Evaporation of materials

NOTE: For better evaporation, the minimum vacuum required is typically a pressure lower than 5×10^{-5} mbar. For all organic materials, the evaporation rate should be kept under 2 Å/s to reduce the roughness and uniformity of the layers. For LiF, the evaporation rate should be less than 0.2 Å/s. Failure to adhere to this may result in nonuniform emissions. If not already done, program the piezoelectric sensor system (which measures the deposition thickness and evaporation rate) with the required parameters, such as 1) material density, 2) Z-factor: an acoustic coupling of material to the sensor, and 3) tooling factor: geometric calibration of the evaporation crucible vs. sample holder. Before using the evaporator, refer to the equipment specifications on how to perform such calibrations, and consult the materials datasheet for the density and Z-factor values for a specific material. Once programmed, and without any evaporation chamber geometry change (tooling factor), the data can be stored for future use with the same materials.

4.1 Insert the substrates (films face-down and after step 3.11 is completed) into the sample holder with the desired evaporation mask (**Figure 4A**).

4.2 Include the necessary crucibles (the geometry depends on the specific evaporator system) and fill each with the necessary materials (LiF, TmPyPb, and Al). A detailed explanation of the thermal evaporation process in OLEDs development can be found in the literature⁴³ and is discussed further in this report.

4.3 Place the substrate holder with samples in the evaporator sample holder (**Figure 4B**). Close the chamber and pump down the evaporator chamber. Follow the respective instructions for the evaporator system.

4.4 Evaporate a film of TmPyPb with a thickness of 40 nm. Evaporate 2 nm of LiF and 100 nm of Al, sequentially. For the evaporation, follow the published procedure⁴³.

NOTE: The final structure is represented in **Figure 4C**. In the current work, devices are not encapsulated. For long-term experiments, encapsulation should be performed, which is not the focus here.

5. Device characterization

NOTE: To characterize the final device, use a highly sensitive voltage meter, luminance meter, and spectrometer. If there is an integrating sphere, use it. Otherwise, place the luminance meter perpendicularly to the OLED surface emission at a distance indicated by the manufacturer and dependent on the focus lens. If not using an integrating sphere, it can be assumed that the OLED device emission follows a Lambertian profile for the efficiency calculation. Here, the plotted brightness does not correspond to the measured under an integrating sphere (thus, it will be at least π times less).

5.1 Insert the fabricated OLED device in the testing holder and make the electrical contacts for the desired pixel. Measure the current (I), applied voltage (V), and brightness (L). Complete details about the experimental setup have been explained previously⁴³.

5.2 With a spectrometer, measure the electroluminescence spectra (EL) at different applied voltages in a range corresponding to the dynamic range of the OLED operation⁴⁴. Take at least three to four spectra. Here, applied voltages of 5 V, 10 V, and 15 V are used.

5.3 Using the necessary software, calculate the current density (J), current efficiency (μ_c candela/Ampere), power efficiency (η_p , lumen/Watt), and external efficiency (EQE). With the electroluminescence spectra, determine the CIE color coordinates. Suitable information on how to calculate all these figures of merit have been described previously⁴⁴.

5.4 Plot the indicated data. Perform a critical analysis of the results in terms of efficiencies and brightness. See the electroluminescence spectra and attempt to establish a model to understand the results.

REPRESENTATIVE RESULTS:

Figure 5 shows the main results for the fabricated device. The turn-on voltage was extremely low (~ 3 V), which is an interesting result for a two organic layer device. The maximum brightness was around 8,000 cd/m² without using an integrating sphere. The maximum values for η_c , η_p , and EQE were around 16 cd/A, 10 lm/W, and 8%, respectively. Although the results are not the best figures of merits for this TADF emitter, they were the best found in such a simple device structure using this emitter via the solution process method.

A maximum EQE of 14.9% was reported in a five-layer thermally evaporated OLED for the same emitter⁴². Importantly, it was observed that the EQE showed a relatively low roll-off behavior (near 7.5% for $L = 100$ cd/m² and $\sim 6\%$ for $L = 1000$ cd/m²), and such roll-off values are the best achieved for this specific TADF emitter⁴². This means that the concept employed for modulating the EML's electrical properties using solution deposition appears to be effectively valid. Some degradation was observed for applied voltages higher than 15 V, which corresponds to the well-known breaking of chemical bonds due to a high electrical carrier density.

The explanation of these results is interesting. Following the concepts and analysis described in the introduction, an electrically balanced and efficient device was obtained, despite the simple structure. With the composition in the EML, modulation of the electrical mobility was calculated to obtain a carrier profile adequate to the best exciton recombination possible. Two simple n-type- or p-type-only devices were prepared following a published procedure⁴⁵, and the mobilities for the active layer were $\mu_n = 6.27 \times 10^{-8} \text{ cm}^2 \text{ V}^{-1} \text{ s}^{-1}$ and $\mu_p = 4.76 \times 10^{-7} \text{ cm}^2 \text{ V}^{-1} \text{ s}^{-1}$.

With solution deposition, a simple electrically balanced device can be achieved, as the electrical properties of the EML can be modulated from correct adjustments and tuning of

the deposition parameters. Depending on the emitters to be tested, this concept can be easily adapted for further development of solution-processed OLEDs.

FIGURE LEGENDS:

Figure 1: Protocol schematic. The used patterned substrates with the ITO strips. In each substrate, six OLEDs with individual areas of 4 mm² were produced. A simple schematic of the deposition process using the spin coater technique is shown. The main area of the deposited film shows the regions to be cleaned to allow the electrical contacts to be precisely positioned when evaporated.

Figure 2: Typical spin coater calibration curve. In this case, and for the active layer, a fixed time of 60 s is used.

Figure 3: AFM image of PVK:OXD-7:2PXZ-OXD (10% wt) 50 nm thin film from chlorobenzene solution. The film was deposited using spin coating as described in the protocol. The RMS value is only 0.309 nm.

Figure 4: Evaporation schematic. (A) Evaporation mask that is adjusted on top of the deposited films. Usually, they are predesigned for specific supports. (B) Schematic of the evaporation chamber with different crucibles. The type, number, and location depend on the specific equipment. The sensors for thickness measurements are placed near the crucibles. On top, the sample holder accommodates the substrate holder with masks. (C) Final schemes (and typical photography) of the produced OLED.

Figure 5: Main figures of merit of the produced green OLEDs. (A) The usual current density (J), applied voltage (V), and brightness (L). (B) Current and power efficiency as a function of current density. (C) The EQE as a function of brightness to evaluate the roll-off. (D) The electroluminescence spectra at 10 V (including the image of the OLEDs).

DISCUSSION:

The protocol used here to fabricate an efficient OLED in a simple device structure is relatively simple. The electrical mobility is not only modulated by the material composition of a device layer but also critically depends on film morphology. Preparation of the solutions and a suitable choice of solvent and concentration are important. No material aggregation can occur, implying complete solubility at the nanometric scale. It is also important to observe the viscosity of the solution. A high viscosity leads to a high contact angle of the solution on the substrate, and the opposite is also possible. In both cases, a nonhomogeneous film can be formed by spin coating. Additionally, starting the spin coater rotation before dropping the solution should be avoided. Finally, an automatic system for dropping the solution in the spin coater is an option, which is advantageous for good thin film deposition. Otherwise, it is necessary to guarantee that the micropipette remains as perpendicular as possible (related with substrate) when dropping the solution. Furthermore, it must be removed immediately when all solution is dropped to avoid extra small drops when the spin coater starts.

As mentioned in the introduction, not all materials can be easily deposited using the

solution process. Fortunately, most devices can be fabricated using the protocol described here. Further improvement of the figures of merit can be achieved, which is strongly dependent on good film formation (even at the molecular stacking scale). The overall electrical properties depend on this. Besides the simplicity of the method, absolute reproducibility of the device using spin coating methods is nearly 50% due to human error. Also, it cannot be used for large area substrates.

Finally, all steps described in the protocol can be viewed as the common framework for producing stable, efficient, and simple OLEDs. Considering the trend toward printed electronics, this work is of major importance for future applications.

ACKNOWLEDGMENTS:

The authors would like to acknowledge the “EXCILIGHT” Project from the European Union’s Horizon 2020 research and innovation program under the Marie Skłodowska-Curie grant agreement No 674990. This work was also developed within the scope of the project i3N, UIDB/50025/2020 & UIDP/50025/2020, financed by national funds through the FCT/MEC.

DISCLOSURES:

The authors have nothing to disclose.

REFERENCES:

1. Tang, C. W., VanSlyke, S. A. Organic electroluminescent diodes. *Applied Physics Letters*. **51** (12), 913-915 (1987).
2. Pereira, D. D. S., Monkman, A. P. Methods of Analysis of Organic Light Emitting Diodes. *Display and Imaging*. **2**, 323-337 (2017).
3. Kumar, M., Ribeiro, M., Pereira, L. New Generation of High Efficient OLED Using Thermally Activated Delayed Fluorescent Materials. In Light-Emitting Diode-An Outlook On the Empirical Features and Its Recent Technological Advancements. *IntechOpen*. (2018).
4. Baldo, M. A. et al. Highly efficient phosphorescent emission from organic electroluminescent devices. *Nature*. **395** (6698), 151 (1998).
5. Uoyama, H., Goushi, K., Shizu, K., Nomura, H., Adachi, C. Highly efficient organic light-emitting diodes from delayed fluorescence. *Nature*. **492** (7428), 234 (2012).
6. Baldo, M., Lamansky, S., Burrows, P., Thompson, M., Forrest, S. Very high-efficiency green organic light-emitting devices based on electrophosphorescence. *Applied Physics Letters*. **75** (1), 4-6 (1999).
7. Adachi, C., Baldo, M. A., Thompson, M. E., Forrest, S. R. Nearly 100% internal phosphorescence efficiency in an organic light-emitting device. *Journal of Applied Physics*. **90** (10), 5048-5051 (2001).
8. Tsuzuki, T., Nakayama, Y., Nakamura, J., Iwata, T., Tokito, S. Efficient organic light-emitting devices using an iridium complex as a phosphorescent host and a platinum complex as a red phosphorescent guest. *Applied Physics Letters*. **88** (24), 243511 (2006).
9. Kwong, R. C. et al. Efficient, saturated red organic light emitting devices based on phosphorescent platinum (II) porphyrins. *Chemistry of Materials*. **11** (12), 3709-3713 (1999).
10. Kalinowski, J., Fattori, V., Cocchi, M., Williams, J. G. Light-emitting devices based on organometallic platinum complexes as emitters. *Coordination Chemistry Reviews*. **255** (21-22), 2401-2425 (2011).
11. Tanaka, D. et al. Ultra high efficiency green organic light-emitting devices. *Japanese*

471 *Journal of Applied Physics*. **46** (1L), L10 (2006).

472 12. Sun, Y. et al. Management of singlet and triplet excitons for efficient white organic
473 light-emitting devices. *Nature*. **440** (7086), 908 (2006).

474 13. Reineke, S. et al. White organic light-emitting diodes with fluorescent tube
475 efficiency. *Nature*. **459** (7244), 234 (2009).

476 14. Helander, M. et al. Chlorinated indium tin oxide electrodes with high work function
477 for organic device compatibility. *Science*. **332** (6032), 944-947 (2011).

478 15. Tao, Y. et al. Multifunctional Triphenylamine/Oxadiazole Hybrid as Host and Exciton-
479 Blocking Material: High Efficiency Green Phosphorescent OLEDs Using Easily Available and
480 Common Materials. *Advanced Functional Materials*. **20** (17), 2923-2929 (2010).

481 16. Lee, C. W., Lee, J. Y. Above 30% external quantum efficiency in blue phosphorescent
482 organic light-emitting diodes using pyrido [2, 3-b] indole derivatives as host materials.
483 *Advanced Materials*. **25** (38), 5450-5454 (2013).

484 17. Endo, A. et al. Efficient up-conversion of triplet excitons into a singlet state and its
485 application for organic light emitting diodes. *Applied Physics Letters*. **98** (8), 42 (2011).

486 18. Endo, A. et al. Thermally activated delayed fluorescence from Sn⁴⁺-porphyrin
487 complexes and their application to organic light emitting diodes—A novel mechanism for
488 electroluminescence. *Advanced Materials*. **21** (47), 4802-4806 (2009).

489 19. Baleizão, C., Berberan-Santos, M. N. Thermally activated delayed fluorescence as a
490 cycling process between excited singlet and triplet states: Application to the fullerenes. *The*
491 *Journal of Chemical Physics*. **126** (20), 204510 (2007).

492 20. Dias, F. B. et al. Triplet harvesting with 100% efficiency by way of thermally activated
493 delayed fluorescence in charge transfer OLED emitters. *Advanced Materials*. **25** (27), 3707-
494 3714 (2013).

495 21. Dias, F. B., Penfold, T. J., Monkman, A. P. Photophysics of thermally activated
496 delayed fluorescence molecules. *Methods and Applications in Fluorescence*. **5** (1), 012001
497 (2015).

498 22. Yersin, H. Highly efficient OLEDs: Materials based on thermally activated delayed
499 fluorescence. *Wiley-VCH*. (2018).

500 23. dos Santos, P. L., Ward, J. S., Bryce, M. R., Monkman, A. P. Using guest–host
501 interactions to optimize the efficiency of TADF Oleds. *The Journal of Physical Chemistry*
502 *Letters*. **7** (17), 3341-3346 (2016).

503 24. Kumar, M., Pereira, L. Effect of the Host on Deep-Blue Organic Light-Emitting Diodes
504 Based on a TADF Emitter for Roll-Off Suppressing. *Nanomaterials*. **9** (9), 1307 (2019).

505 25. Méhes, G., Goushi, K., Potscavage Jr., W. J., Adachi, C. Influence of host matrix on
506 thermally-activated delayed fluorescence: Effects on emission lifetime, photoluminescence
507 quantum yield, and device performance. *Organic Electronics*. **15** (9), 2027-2037 (2014).

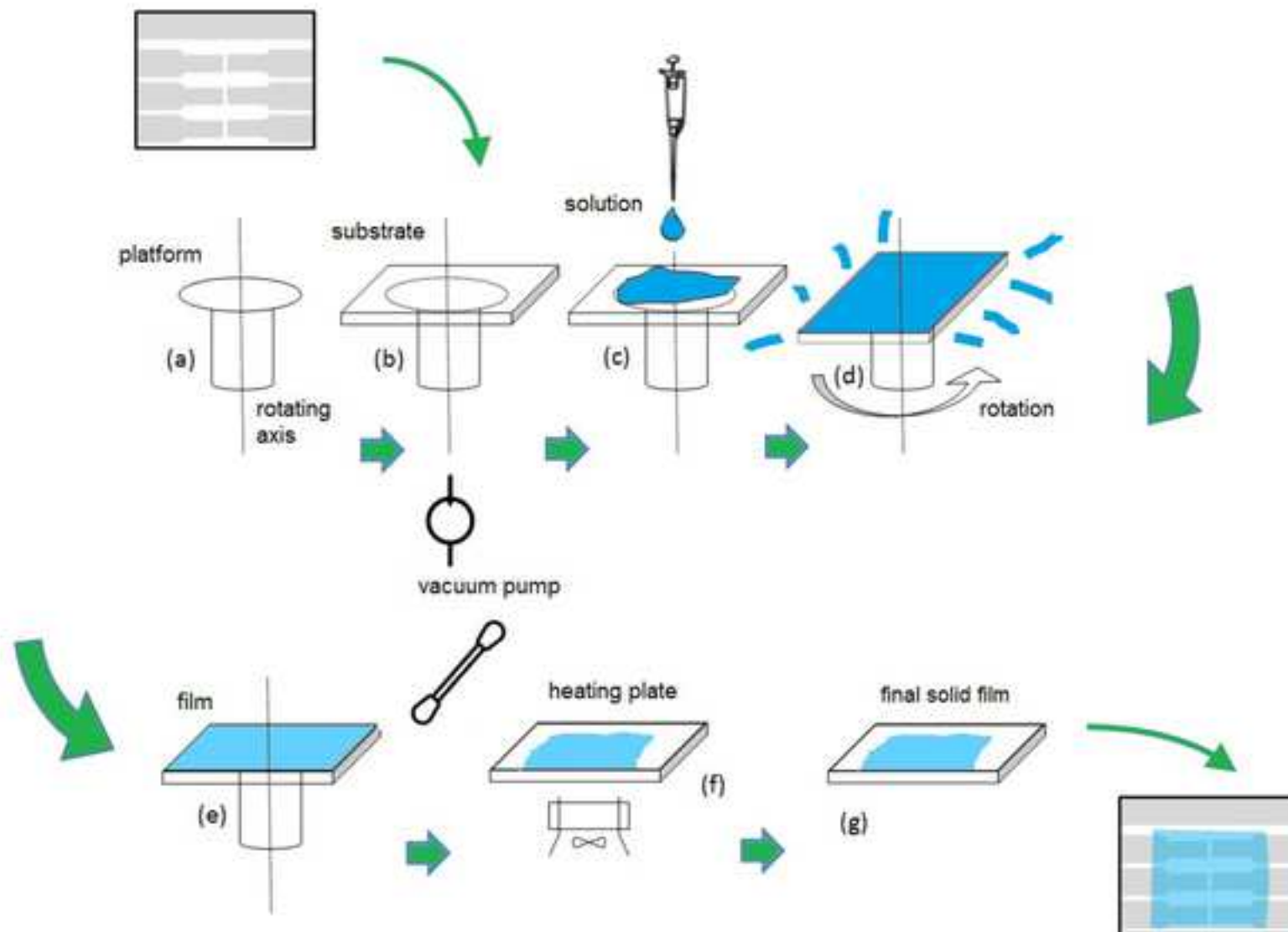
508 26. Yang, Z. et al. Recent advances in organic thermally activated delayed fluorescence
509 materials. *Chemical Society Reviews*. **46** (3), 915-1016 (2017).

510 27. Wong, M. Y., Zysman-Colman, E. Purely organic thermally activated delayed
511 fluorescence materials for organic light-emitting diodes. *Advanced Materials*. **29** (22),
512 1605444 (2017).

513 28. Tsai, K. W., Hung, M. K., Mao, Y. H., Chen, S. A. Solution-Processed Thermally
514 Activated Delayed Fluorescent OLED with High EQE as 31% Using High Triplet Energy
515 Crosslinkable Hole Transport Materials. *Advanced Functional Materials*. 1901025 (2019).

516 29. Lin, T. A. et al. Sky-blue organic light emitting diode with 37% external quantum
517 efficiency using thermally activated delayed fluorescence from spiroacridine-triazine hybrid.

- Advanced Materials*. **28** (32), 6976-6983 (2016).
30. Cho, Y. J., Yook, K. S., Lee, J. Y. High efficiency in a solution-processed thermally activated delayed-fluorescence device using a delayed-fluorescence emitting material with improved solubility. *Advanced Materials*. **26** (38), 6642-6646 (2014).
31. Huang, T., Jiang, W., Duan, L. Recent progress in solution processable TADF materials for organic light-emitting diodes. *Journal of Materials Chemistry C*. **6** (21), 5577-5596 (2018).
32. Kumar, M., Pereira, L. Towards Highly Efficient TADF Yellow-Red OLEDs Fabricated by Solution Deposition Methods: Critical Influence of the Active Layer Morphology. *Nanomaterials*. **10** (1), 101 (2020).
33. Cai, M. et al. High-efficiency solution-processed small molecule electrophosphorescent organic light-emitting diodes. *Advanced Materials*. **23** (31), 3590-3596 (2011).
34. Amruth, C., Szymański, M. Z., Łuszczńska, B., Ulański, J. Inkjet printing of super Yellow: Ink Formulation, Film optimization, oLEDs Fabrication, and transient electroluminescence. *Scientific Reports*. **9** (1), 1-10 (2019).
35. Abbel, R. et al. Toward high volume solution based roll-to-roll processing of OLEDs. *Journal of Materials Research*. **32** (12), 2219-2229 (2017).
36. Hast, J. et al. In 18.1: Invited Paper: Roll-to-Roll Manufacturing of Printed OLEDs, SID Symposium Digest of Technical Papers, *Wiley Online Library*. 192-195 (2013).
37. Chang, S. C. et al. Multicolor organic light-emitting diodes processed by hybrid inkjet printing. *Advanced Materials*. **11** (9), 734-737 (1999).
38. Singh, M., Haverinen, H. M., Dhagat, P., Jabbour, G. E. Inkjet printing—process and its applications. *Advanced Materials*. **22** (6), 673-685 (2010).
39. Villani, F. et al. Inkjet printed polymer layer on flexible substrate for OLED applications. *The Journal of Physical Chemistry C*. **113** (30), 13398-13402 (2009).
40. Choi, K.-J., Lee, J.-Y., Shin, D.-K., Park, J. Investigation on slot-die coating of hybrid material structure for OLED lightings. *Journal of Physics and Chemistry of Solids*. **95**, 119-128 (2016).
41. Geffroy, B., Le Roy, P., Prat, C. Organic light-emitting diode (OLED) technology: materials, devices and display technologies. *Polymer International*. **55** (6), 572-582 (2006).
42. Lee, J. et al. Oxadiazole- and triazole-based highly-efficient thermally activated delayed fluorescence emitters for organic light-emitting diodes. *Journal of Materials Chemistry C*. **1** (30), 4599-4604 (2013).
43. Monkman, A., Data, P. Production and Characterization of Vacuum Deposited Organic Light Emitting Diodes. *Journal of Visualized Experiments*. (141), (2018).
44. Pereira, L. F. Organic light emitting diodes: The use of rare earth and transition metals. *Pan Stanford*. (2012).
45. Kumar, M., Pereira, L. Mixed-Host Systems with a Simple Device Structure for Efficient Solution-Processed Organic Light-Emitting Diodes of a Red-Orange TADF Emitter. *ACS Omega*. **5** (5), 2196-2204 (2020).



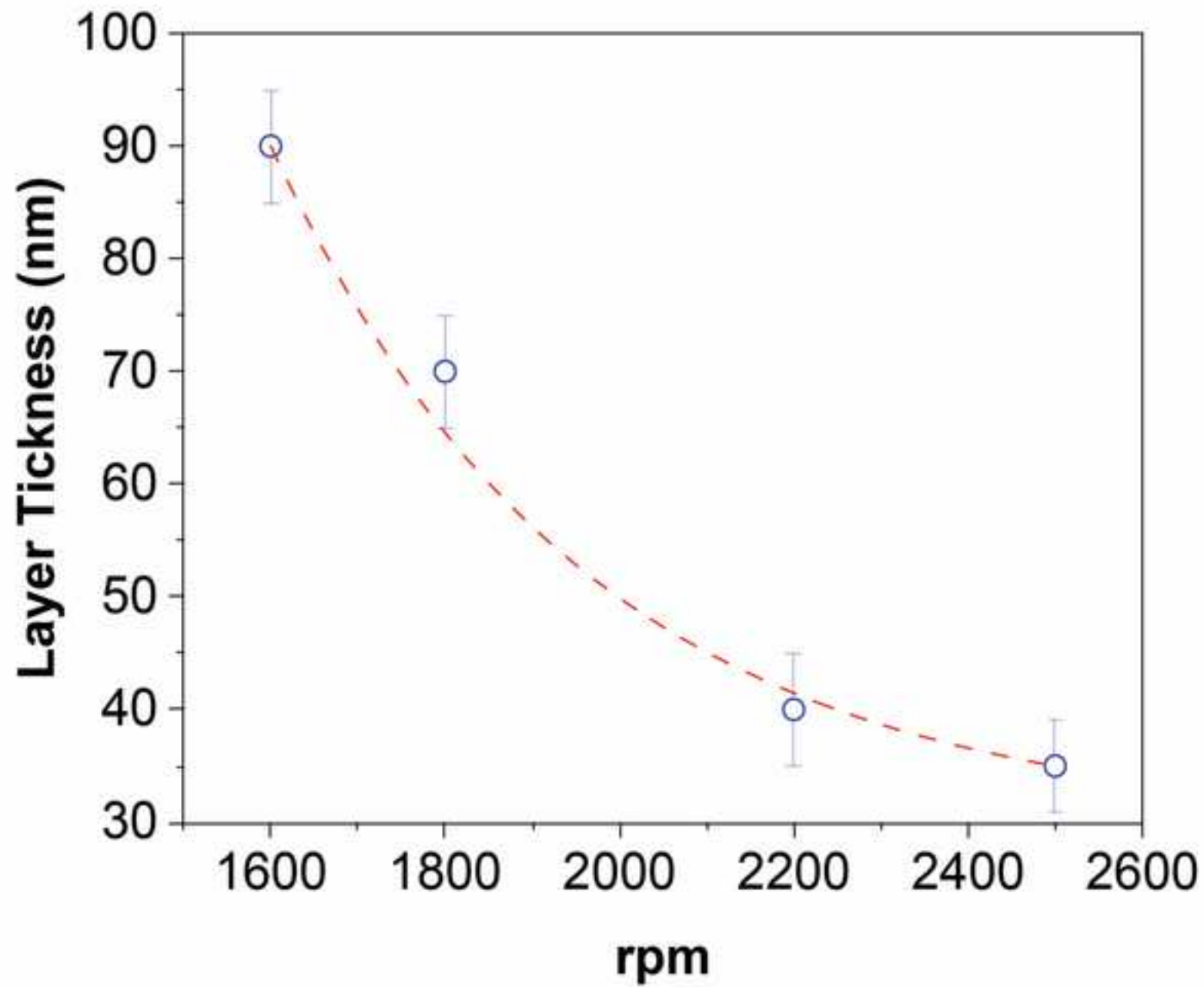
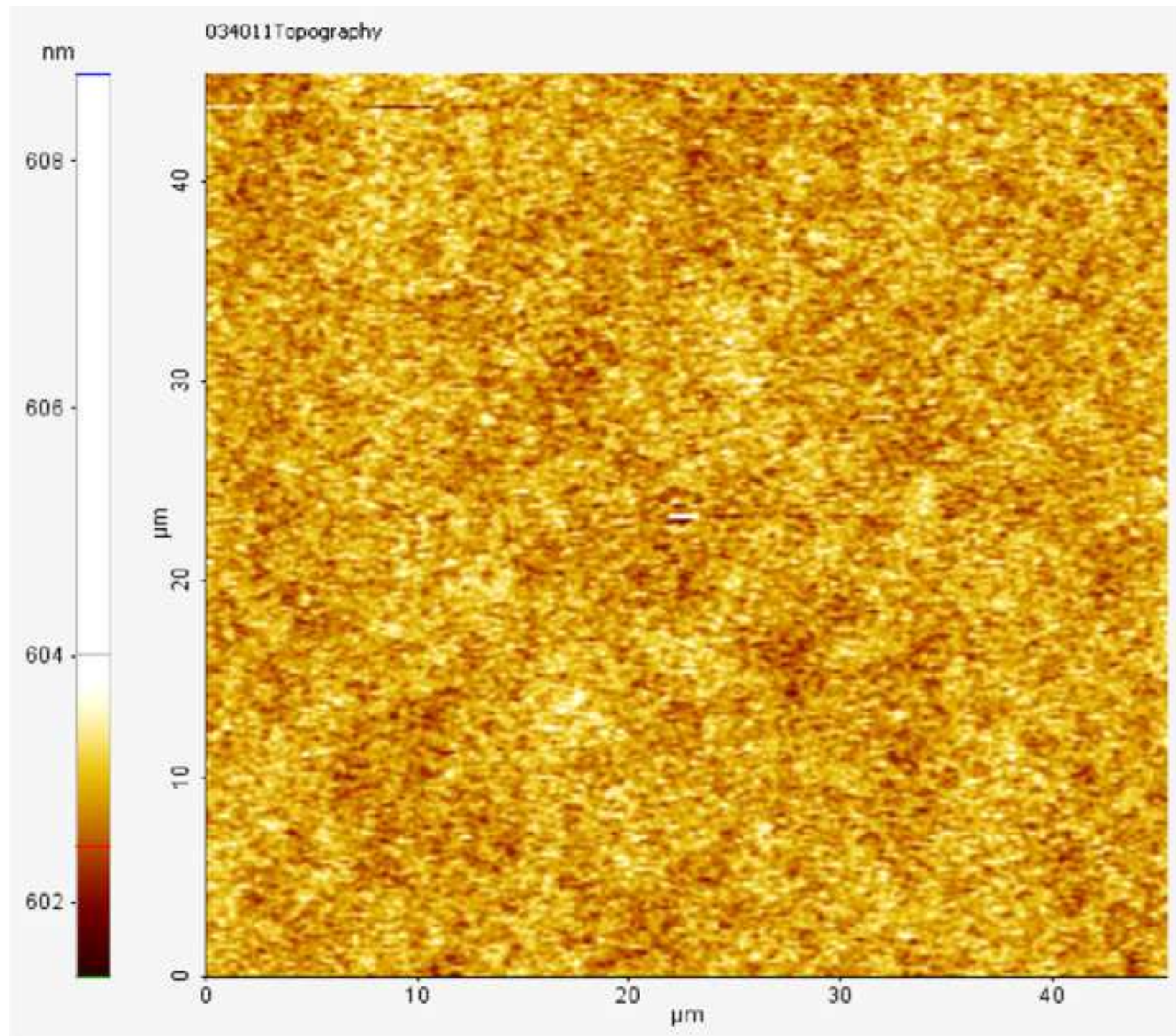


Figure3

[Click here to access/download;Figure;Figure 3.psd](#)



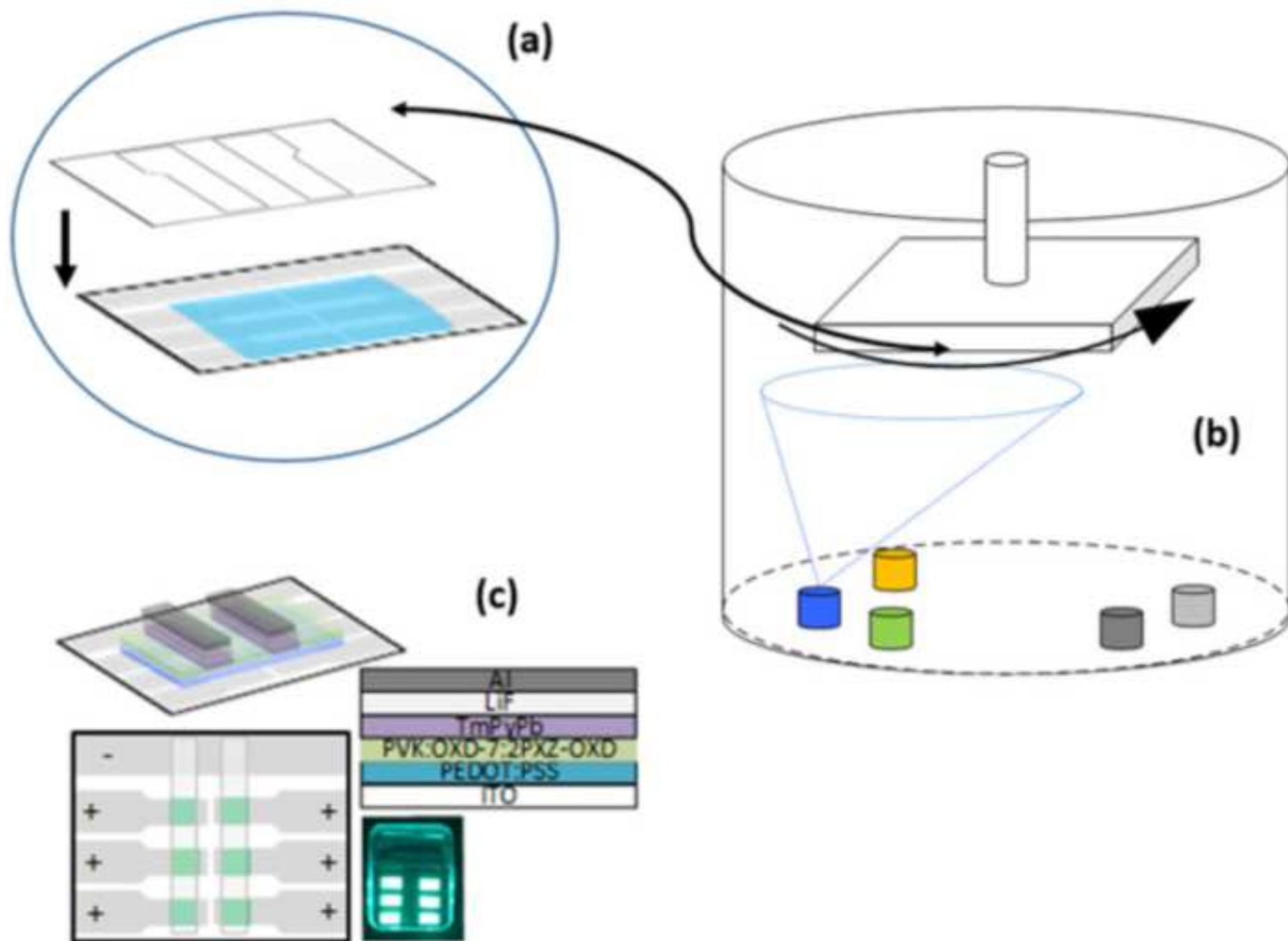
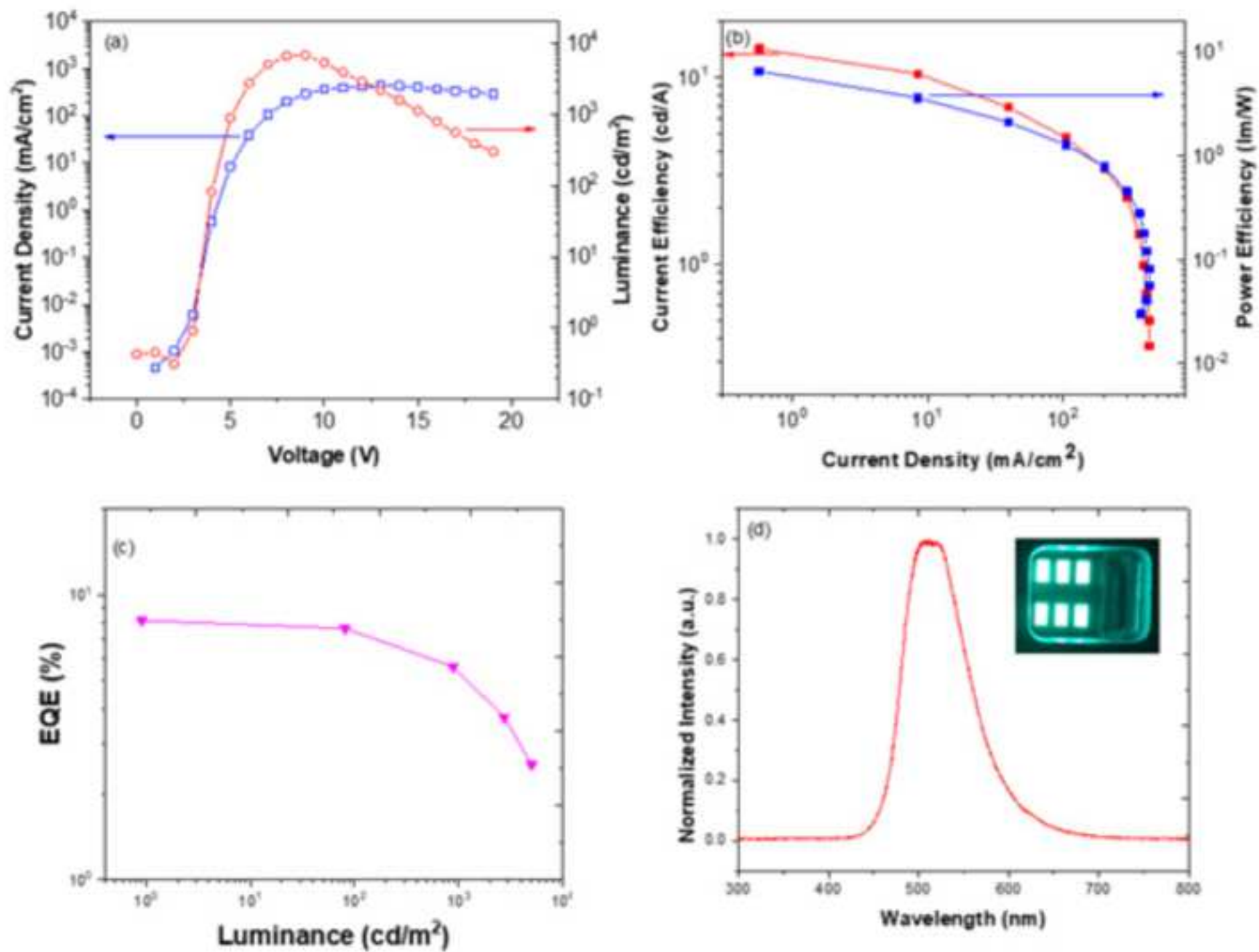


Figure 5

[Click here to access/download;Figure;Figure 5.psd](#)

Name of Material/ Equipment	Company	CAS Number
2PXZ-OXD (2,5-bis(4-(10H-phenoxazin-10-yl)phenyl)-1,3,4-oxadiazole)	Lumtec ltd	1447998-13-1
Aluminum (99.999%)	Alfa Aesar	7429-90-5
Acetone (99.9%)	Sigma Aldrich	67-64-1
Hellmanex	Ossila	7778-53-2
Isopropyl alcohol	Sigma Aldrich	67-63-0
ITO patterned substrates	Ossila	65997-17-3
Lithium Fluoride (99.99%)	Sigma Aldrich	7789-24-4
OXD-7 (1,3-Bis[2-(4-tert-butylphenyl)-1,3,4-oxadiazole-5-yl]benzene)	Ossila	138372-67-5
PEDOT: PSS (Poly(3,4-ethylenedioxythiophene) polystyrene sulfonate)	Ossila	155090-83-8
PVK (Polyvinylcarbazole) (average Mn 25,000-50,000)	Sigma Aldrich	25067-59-8
TmPyPb (1,3,5-Tri(m-pyridin-3-ylphenyl)benzene)	Ossila	138372-67-5

Comments/Description

JoVE Manuscript JoVE61071R1

Answer to the Referrers / Editorial Comments

Editorial comments:

1. Please employ professional copy-editing services as the language in the manuscript is not publication grade. Please note that the poor language prevents a thorough review of the manuscript.

Response: Revised

2. Please upload each figure individually as an image file.

Response: will be done

3. 2.1: What does Ossila refer to? Please use a numerical reference from the Reference section.

Response: Correct in the manuscript

4. The grammar is severely compromising the clarity of the protocol. Please revise.

Response: Revised

5. Please discuss limitations of the protocol in the discussion section.

Response: A sentence was added pointing the most know limitatios.

Reviewers' comments:

Reviewer #2:

Manuscript Summary: Accept

Reviewer #3:

Manuscript Summary:

The authors of the manuscript have greatly improved their text rendering it to be nearly ready for publication. The text is now supported by sufficient citation. Most of reviewers' suggestions have been applied with benefit to the manuscript. In reviewer's opinion the authors discussed the topic of spin-coating sufficiently and in a sound and balanced manner, pointing out important issues and reducing discussion of irrelevant topics.

However, there still exist numerous editorial errors and the language of the manuscript is insufficient in some places, although it greatly improved from the previous version. In general these issues are to be dealt with in editorial revision as of the rules of JoVE, thus no further peer-review is necessary.

Minor Concerns:

The authors use term "weighing machine", should this be scales or balance?

Response: A scale-machine. This information was added in the manuscript

The authors should consider presenting comments to the protocol step as a note, i.e. below the relevant step. In current layout the note and action to be done in the step are blended together which may be difficult to follow by readers.

Response: Done in the manuscript

References 43 and 44 are the same.

Response: Corrected

Fig 1, step g: the text seems not to be fully visible

Response: corrected